Japanese Journal of Applied Physics
Vol. 46, No. 47, 2007, pp. L1176–L1178



# Quantum-Size Effect in Uniform Ge–Sn Alloy Nanodots Observed by Photoemission Spectroscopy

Yasuo NAKAYAMA[1*], Keiko TAKASE[2], Toru HIRAHARA[1,2], Shuji HASEGAWA[1,2], Taichi OKUDA[3], Ayumi HARASAWA[3], Iwao MATSUDA[1,3], Yoshiaki NAKAMURA[1,4], and Masakazu ICHIKAWA[1,4]

[1]*Core Research for Evolutional Science and Technology (CREST), Japan Science and Technology Agency (JST), Kawaguchi, Saitama 332-0012, Japan*
[2]*Department of Physics, Graduate School of Science, The University of Tokyo, Tokyo 113-0033, Japan*
[3]*Synchrotron Radiation Laboratory, Institute for Solid State Physics, The University of Tokyo, Kashiwa, Chiba 277-8581, Japan*
[4]*Quantum-Phase Electronics Center, Department of Applied Physics, Graduate School of Engineering, The University of Tokyo, Tokyo 113-8656, Japan*

(Received September 11, 2007; revised October 7, 2007; accepted October 29, 2007; published online November 30, 2007)

Nanodots of super-saturated Ge–Sn alloy formed on a Si substrate covered with a $SiO_2$ monolayer were investigated by photoemission spectroscopy. Core-level photoemission results indicated that the stoichiometry of the nanodots was uniform at an intended ratio without Sn segregation. Quantum size effect was also proved by valence-band photoemission on the present GeSn nanodots. [DOI: 10.1143/JJAP.46.L1176]

KEYWORDS: quantum size effect, GeSn nanodots, photoemission, optoelectronics

A GeSn alloy has been considered as a candidate for light-emitting devices composed of group-IV semiconductors because it will change into a direct-gap semiconductor when the composition ratio of Sn is larger than the critical ratio of around 0.12.[1–3] However Sn tends to segregate from Ge due to limited solid-solubility,[4] which makes it difficult to produce a uniform GeSn alloy with an intended stoichiometry. Large lattice mismatch between the GeSn alloy and Si is also a significant disadvantage for using this material as an optoelectronics device combined with conventional Si-based electronics, because it prevents the alloy from crystallizing epitaxially without dislocations onto Si substrates. Some attempts have been made against these deficiencies to produce uniform GeSn alloys through non-equilibrium growth methods; e.g. low-temperature molecular beam epitaxy,[2] magnetron sputtering,[3] and chemical vapor deposition.[5] In addition, since the gap-width (0.3–0.5 eV) of the direct-gap GeSn alloys is narrower compared to the optical-communication wave-length (1.5 μm; ~0.8 eV), band-gap widening by quantum-size effect is anticipated to apply them as light-emitting devices of high efficiency.

Recently, hemispherical nanodots of a super-saturated GeSn alloy were successfully produced by co-deposition of Ge and Sn on a Si substrate covered with a $SiO_2$ monolayer with pre-deposited Ge nuclei.[6,7] The size of them is smaller than 10 nm and it is controllable by changing the coverage (deposition amount). Moreover, high-resolution transmission electron microscopy (TEM) images indicated that the crystal lattice in the nanodots is thoroughly epitaxial to the Si substrate with neither strain nor dislocations.[7] The above results show that the present GeSn nanodot is a promising candidate for optoelectronics application if both of the following requirements are satisfied; segregation of Sn does not take place, and the nanodots actually exhibit quantum-size effect. The former point is needed to realize a direct-gap condition. No surface segregation of Sn was implied by atomic-number dependent contrast of scanning TEM imaging although the spatial resolution was limited.[7] Concerning the latter point, while scanning tunneling spectroscopy results showed band-gap narrowing as dot-size grows,[6] uncertainty originating from a tip-induced field effect cannot be excluded.

In the present study, we conducted core-level and valence-band photoemission spectroscopy (PES) of the GeSn nanodots on the $SiO_2$ monolayer for the sake of confirming no Sn segregation and occurrence of the quantum-size effect simultaneously on identical nanodot arrays.

The Si substrate was cut from a mirror polished *n*-type Si(111) wafer (1–10 Ω cm). A clean Si(111) $7 \times 7$ surface was prepared by repeated cycles of resistive heating up to 1200 °C after careful degassing at *ca.* 350 °C in ultrahigh vacuum (UHV). The current–temperature relationship of the Si substrate was calibrated down to 200 °C by an infrared pyrometer. Ge and Sn were deposited from tube cells hollowed out of graphite rods heated by surrounding tungsten filaments insulated by alumina tubes. The evaporation rates of Ge and Sn were set at 0.22 BL/min (bilayers per minute) and 0.04 BL/min, respectively, which were separately estimated from disappearance of $7 \times 7$ low energy electron diffraction patterns at room temperature (RT) for Ge and at 400 °C for Sn, which correspond to 1/4 BL for Ge[8] and 1/6 BL for Sn[9] (1 BL = $1.57 \times 10^{15}$ $cm^{-2}$). We fabricated epitaxial GeSn nanodots by a method discovered by Nakamura *et al.*[7] which is schematically drawn in Fig. 1. At first, a 0.3-nm-thick $SiO_2$ layer over the Si(111) was generated by oxygen exposure ($2 \times 10^{-4}$ Pa) onto the surface in increasing the sample temperature up to 630 °C for 10 min (process I in Fig. 1).[10] Pre-deposition of 1 BL Ge onto the $SiO_2$ monolayer kept at 650 °C yields sub-nanometer sized voids penetrating though the $SiO_2$ monolayer (II),[10] which act as the nuclei of subsequent nanodot growth. Finally, a shutter of the Sn cell was opened immediately after the heating current to the Si substrate was flopped down to a value corresponding to 200 °C (III). PES spectra were obtained by an angle-integrated electron spectrometer (VG; CLAM1) on a vacuum-ultra-violet beamline BL-18A at Photon Factory (PF) in High Energy Accelerator Research Organization (KEK), Japan.

Total coverage dependence of the dot-size was estimated from scanning tunneling microscopy (STM) images.[7] ["Total" coverage counts simultaneously deposited amounts of Ge and Sn totally but excludes the pre-deposited Ge (1 BL), hereafter.] In the present case, we have to know "typical" dot-size for each coverage that makes the greatest contribution on PES spectra. Such dot-size can be decided from a distribution of appearance frequencies multiplied by volumes of the corresponding dot radii.[11,12] Figure 2(a) displays the size distributions of the dot arrays, and by fitting

*Present address: Center for Frontier Science, Chiba University, Chiba 263-8522, Japan. E-mail address: nkym@restaff.chiba-u.jp

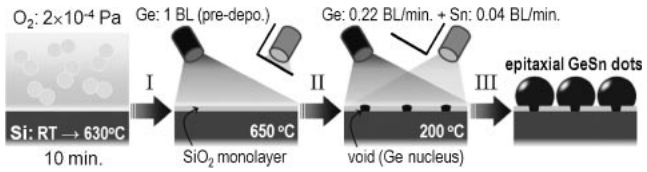


Fig. 1. A schematic drawing of the procedure for fabricating the epitaxial GeSn nanodots.

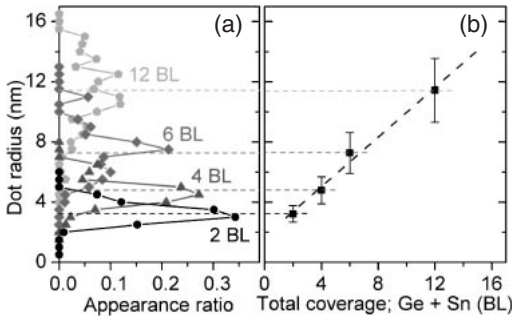


Fig. 2. (a) Normalized histograms of appearance frequencies multiplied by corresponding volume of the GeSn nanodots estimated from STM images. Thick lines show fitting curves of the size distributions with the Gaussian function. (b) The "typical" radius (the Gaussian center) plotted as a function of the total coverage. A broken line shows a fitting line of the plot. Error-bars correspond to the Gaussian full-widths of the half-maxima.

each of them with a Gaussian curve, the "typical" dot radii are estimated as a function of the total coverage [Fig. 2(b)]. The radius seems to grow almost linearly to the coverage, when the total coverage is greater than 2 BL, similarly to the case of Ge nanodots.[11,12)]

Since the ratio of deposition rate of Ge and Sn is roughly 0.85 : 0.15, composition ratio should also be this value if the sticking probability is the same for Ge and Sn. On the other hand, stoichiometry of the nanodots can be evaluated from peak intensities of Ge and Sn core-level PES spectra. We estimated the *actual* composition ratio of Ge and Sn for each dot radius from peak intensities of Ge 3d and Sn 4d PES spectra obtained by photons of 55 eV (Fig. 3), in which we used 2 and 50 Mbarn for photo-ionization cross-section of Ge 3d and Sn 4d levels, respectively.[13)] Although the data show apparent scattering, the estimated stoichiometry looks staying around the intended ratio of (Ge : Sn) = (0.85 : 0.15) independent of the dot radius. For the present condition, the inelastic mean free path of the photoelectrons emitted from both Ge 3d and Sn 4d orbitals are around 1 nm. Thus, if the deposited Sn segregates and covers the surface of the nanodots, the ratio of Sn peak should appear greater as the dot-size grows larger than 1 nm. Uniformity of observed stoichiometry (or rather suppression of the Sn ratio for the largest dot-size) therefore suggests no Sn segregation at surfaces of the nanodots. In addition, Sn 4d peak can be fitted as a single component of a reasonable peak-width (0.67 eV) by using reported spin-orbit splitting and blanching ratio,[14)] as shown in the inset of Fig. 3. It also points out uniform distribution of Sn atoms in the alloy dots, considering that even a faint difference in adsorption site of Sn on Ge surface makes an apparent chemical shifts.[14–16)] The aforementioned scanning TEM results[7)] are also supported by these results.

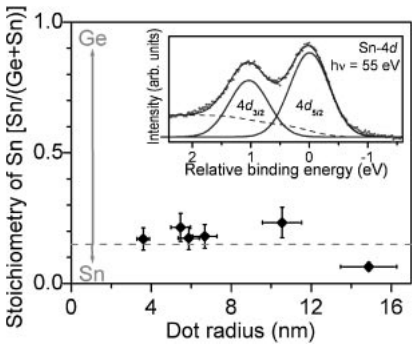


Fig. 3. Composition ratio of Sn in the GeSn nanodots of each dot-radius evaluated from peak intensities of Ge 3d and Sn 4d PES. A gray broken line shows the intended stoichiometry [(Ge : Sn) = (0.85 : 0.15)]. Inset: Sn 4d PES spectra of the GeSn nanodots ($r = 5.4$ nm; total coverage is 6 BL). Dots, a broken line, thick solid lines, and a thin solid line show the experimental data, a Shirley-type background curve, Gaussian fitting curves, and a sum of the fitting curves, respectively.

Figure 4(a) shows valence band PES spectra of the $SiO_2$ monolayer and the GeSn nanodot arrays of noted dot-sizes obtained at the photon energy of 21.2 eV. The Fermi-level position ($E_F$) was decided from a tantalum clamp plate which was in good electrical contact with the sample. Wide range spectra of the $SiO_2$ monolayer (not shown) looks good agreement with our previous reports,[11,12)] which indicates that the valence band maximum (VBM) of the $SiO_2$ monolayer ($E^{VBM}_{SiO_2}$) states around 5 eV from $E_F$. Taking into consideration that mean free path of the present photoelectron (a few nm) is much longer than the thickness of the oxide layer, PES signals existing within energy range between $E^{VBM}_{SiO_2}$ and $E_F$ is attributed to bulk states of the Si(111) substrate.[17)] On the other hand, concerning the PES spectra of the nanodot arrays, no striking features (e.g., peaks) originating from a quantized energy level of the nanodot cannot be found on the spectra probably due to size distribution on each nanodot array as well as limitation of the energy resolution of the experimental apparatus (no better than 0.1 eV). That prevents us from determining absolute position of the quantized energy level [in the present case, the highest occupied state (HOS) of the confined holes]. Energy shift of HOS is however available from change in the "VBM" of each nanodot array. We define VBM as an intersection point of two fitting lines of the spectral tail and background signals, and amounts of energy shift of the VBM ($\Delta E_{VBM}$) compared to $E^{VBM}_{Si}$ is plotted in Fig. 4(b) as a function of inverse dot-radius. The present behavior that the energy position of VBM leaves from $E_F$ as the dot-size becomes smaller (or the inverse dot-radius becomes greater) is characteristic of quantum-size effect.[11,12,17–20)]

We recently revealed that the dot-size dependent shift of the VBM of Ge nanodots is successfully explained as confinement of holes into the nanodots by a harmonic potential barrier.[11,12)] Analytical solution of the quantized energy (corresponding to HOS) of the holes $E_{HOS}$ confined by a spherical harmonic potential is given as;[11,12,17,21,22)]

$$E_{HOS} = \frac{2a_B}{\sqrt{Ry}}\sqrt{\frac{V}{m^*_h}}\frac{1}{r} = E_0 - \Delta E_{VBM},$$

where Ry is the atomic Rydberg and $a_B$ is the atomic Bohr radius. ($E_0$ is an energy reference and it is unnecessary to be

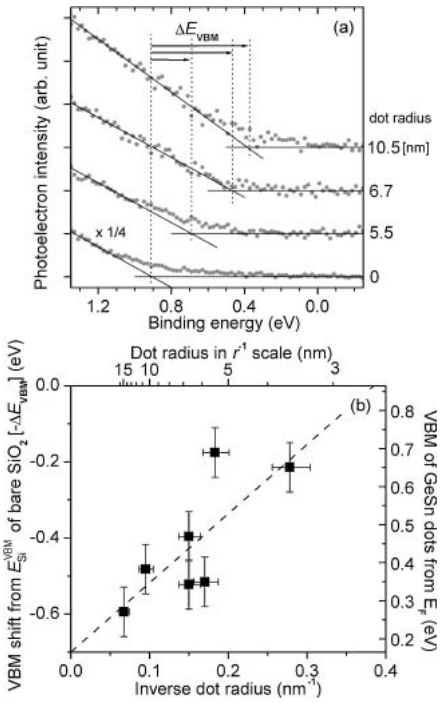


Fig. 4. (a) Valence-band PES spectra of the GeSn nanodots of noted coverages presented together with that of the bare $SiO_2$ monolayer ($r = 0$ nm). Solid lines show fitting lines of spectral tails and backgrounds. (b) Energy shift of the VBM of the GeSn nanodots ($-\Delta E_{VBM}$) from that of the bulk Si underneath the bare $SiO_2$ monolayer plotted as a function of inverse dot-radii. Least-squares fit by $-\Delta E_{VBM} \propto r^{-1}$ is displayed with a broken line.

determined in the present procedure.) On the other hand, one can evaluate the potential barrier height ($V$) from a gradient of the $1/r$–$E_{VBM}$ plot. Strictly speaking, however, we can only determine $\sqrt{V/m_h^*}$ in the present case because the effective-mass of the holes ($m_h^*$) in such super-saturated Ge–Sn alloy is unknown. The estimated value for the present results is $\sqrt{V/m_h^*} = 4.7 \pm 1.0\,\mathrm{eV}^{1/2}/{m_0}^{1/2}$. By adopting a reported value for $m_h^*$ which was evaluated from dot-size dependent scanning tunneling spectroscopy on the GeSn nanodots,[6] we obtain the confining potential barrier height $V$ as $2.0 \pm 0.9$ eV. This value is significantly small as a confining barrier height of the present system, which should be ascribed to the valence band offset between Ge–Sn alloy and the $SiO_2$ monolayer ($\sim$4.5 eV). The reduction of the confining barrier is probably ascribed to the subnanometer-sized voids interconnecting the nanodots and the substrate (see Fig. 1). It is interesting to note that the present barrier height is quite equivalent to our previous results on the epitaxial nanodots of pure Ge formed on the $SiO_2$ with the voids,[11,12,17] which indicates that materials composing the nanodots do not influence the confining potential of the interface barrier layer.

The barrier height at the interface plays an essential role on the carrier transport nature between the nanodots and the substrate. Nakamura and coworkers reported quicker escape of an electron confined into the epitaxial Ge nanodot through the reduced potential barrier compared to the non-epitaxial case.[23] We recently revealed that conductivity enhancement on the epitaxial Ge nanodot arrays is realized because carriers generated in the nanodots can pass through the reduced barrier into the substrate to conduct, whereas such carrier provision is prevented for the non-epitaxial case.[24] The present value for the interface barrier height is sufficiently low to realize an improved carrier exchange between the nanodots and the substrate.[24] Since effectual carrier injection into the nanodots is indispensable for device operation, the present results suggest propriety of the GeSn nanodots for future optoelectronics application.

In conclusion, we have conducted core-level and valence-band photoemission spectroscopy on the super-saturated Ge–Sn alloy nanodots formed on the $SiO_2$ monolayer. Core-level PES results indicate that no segregation of Sn occurs in the GeSn nanodots. Quantum size effect was successfully proved in the GeSn nanodots by means of valence-band PES, and estimated confining potential barrier height by the $SiO_2$ monolayer with the voids is quite consistent to our previous results.

This work was performed under the approval of the PF Program Advisory Committee (Proposal No. 2005G089). The authors acknowledge financial support from CREST, JST and the Japan Society for the Promotion of Science (JSPS).

1) D. W. Jenkins and J. D. Dow: Phys. Rev. B **36** (1987) 7994.
2) G. He and H. A. Atwater: Phys. Rev. Lett. **79** (1997) 1937.
3) H. P. L. de Guevara, A. G. Rodríguez, H. N.-Contreras, and M. A. Vidal: Appl. Phys. Lett. **84** (2004) 4532.
4) L. Baldé, B. Legendre, and A. Balkhi: J. Alloys Compd. **216** (1995) 285 [in French].
5) V. R. D'Costa, C. S. Cook, A. G. Birdwell, C. L. Littler, M. Canonico, S. Zollner, J. Kouvetakis, and J. Menéndez: Phys. Rev. B **73** (2006) 125207.
6) Y. Nakamura, A. Masada, and M. Ichikawa: Appl. Phys. Lett. **91** (2007) 013109.
7) Y. Nakamura, A. Masada, S.-P. Cho, N. Tanaka, and M. Ichikawa: to be published in J. Appl. Phys.
8) V. G. Lifshits, A. A. Saranin, and A. V. Zotov: *Surface Phases on Silicon: Preparation, Structures, and Properties* (Wiley, Chichester, U.K., 1994) p. 214.
9) F. Guo, K. Kobayashi, and T. Kinoshita: e-J. Surf. Sci. Nanotechnol. **3** (2005) 350.
10) A. A. Shklyaev, M. Shibata, and M. Ichikawa: Phys. Rev. B **62** (2000) 1540.
11) Y. Nakayama, I. Matsuda, S. Hasegawa, and M. Ichikawa: Appl. Phys. Lett. **88** (2006) 253102.
12) Y. Nakayama, I. Matsuda, S. Hasegawa, and M. Ichikawa: Hyomen Kagaku **27** (2006) 523 [in Japanese].
13) J. J. Yeh and I. Lindau: At. Data Nucl. Data Tables **32** (1985) 1.
14) M. E. Dávila, J. Avila, M. C. Asensio, M. Göthelid, U. O. Karlsson, and G. L. Lay: Surf. Sci. **600** (2006) 3154.
15) R. I. G. Uhrberg, H. M. Zhang, and T. Balasubramanian: Phys. Rev. Lett. **85** (2000) 1036.
16) T.-L. Lee, S. Warren, B. C. C. Cowie, and J. Zegenhagen: Phys. Rev. Lett. **96** (2006) 046103.
17) A. Konchenko, Y. Nakayama, I. Matsuda, S. Hasegawa, Y. Nakamura, and M. Ichikawa: Phys. Rev. B **73** (2006) 113311.
18) V. L. Colvin, A. P. Alivisatos, and J. G. Tobin: Phys. Rev. Lett. **66** (1991) 2786.
19) S. A. Ding, M. Ikeda, M. Fukuda, S. Miyazaki, and M. Hirose: Appl. Phys. Lett. **73** (1998) 3881.
20) T. van Buuren, L. N. Dinh, L. L. Chase, W. J. Siekhaus, and L. J. Terminello: Phys. Rev. Lett. **80** (1998) 3803.
21) J. Adamowski, M. Sobkowicz, B. Szafran, and S. Bednarek: Phys. Rev. B **62** (2000) 4234.
22) M. Ciurla, J. Adamowski, B. Szafran, and S. Bednarek: Physica E **15** (2002) 261.
23) Y. Nakamura, M. Ichikawa, K. Watanabe, and Y. Hatsugai: Appl. Phys. Lett. **90** (2007) 153104.
24) Y. Nakayama, S. Yamazaki, H. Okino, T. Hirahara, I. Matsuda, S. Hasegawa, and M. Ichikawa: Appl. Phys. Lett. **91** (2007) 123104.